

This article was downloaded by:

On: 25 January 2011

Access details: *Access Details: Free Access*

Publisher *Taylor & Francis*

Informa Ltd Registered in England and Wales Registered Number: 1072954 Registered office: Mortimer House, 37-41 Mortimer Street, London W1T 3JH, UK



Liquid Crystals

Publication details, including instructions for authors and subscription information:

<http://www.informaworld.com/smpp/title~content=t713926090>

The semi-phenomenological model of antiferroelectricity in chiral smectic liquid crystals II. The phase transitions and phase diagrams

S. Pikin; M. Gorkunov; D. Kilian; W. Haase

Online publication date: 06 August 2010

To cite this Article Pikin, S. , Gorkunov, M. , Kilian, D. and Haase, W.(1999) 'The semi-phenomenological model of antiferroelectricity in chiral smectic liquid crystals II. The phase transitions and phase diagrams', *Liquid Crystals*, 26: 8, 1115 – 1122

To link to this Article: DOI: 10.1080/026782999204138

URL: <http://dx.doi.org/10.1080/026782999204138>

PLEASE SCROLL DOWN FOR ARTICLE

Full terms and conditions of use: <http://www.informaworld.com/terms-and-conditions-of-access.pdf>

This article may be used for research, teaching and private study purposes. Any substantial or systematic reproduction, re-distribution, re-selling, loan or sub-licensing, systematic supply or distribution in any form to anyone is expressly forbidden.

The publisher does not give any warranty express or implied or make any representation that the contents will be complete or accurate or up to date. The accuracy of any instructions, formulae and drug doses should be independently verified with primary sources. The publisher shall not be liable for any loss, actions, claims, proceedings, demand or costs or damages whatsoever or howsoever caused arising directly or indirectly in connection with or arising out of the use of this material.

The semi-phenomenological model of antiferroelectricity in chiral smectic liquid crystals†

II. The phase transitions and phase diagrams

S. PIKIN*, M. GORKUNOV

Institute of Crystallography, Russian Academy of Sciences, Leninskii prosp. 59,
117333 Moscow, Russia

D. KILIAN and W. HAASE

Institut für Physikalische Chemie, Technische Universität Darmstadt,
Petersenstr. 20, 64287 Darmstadt, Germany

(Received 19 December 1998; accepted 22 February 1999)

In the framework of the model of short pitch modes (SPM) developed for chiral smectics with inclined molecules, the phase transitions and diagrams in antiferroelectric systems are described. It is shown that the families of antiferro- and ferri-electric phases are controlled by a few physical parameters such as the smectic correlation length and the chirality parameter. The sequences of antiferro- and ferri-electric states are explained as being dependent on the interactions between SPM and the conventional long pitch mode (LPM), the ferrielectric states being described in terms of the obvious coexistence of LPM and several SPM.

1. Introduction

Along with the models [1–8] applied for the consideration of very complicated problems related to antiferroelectric structures and the properties of new liquid crystalline substances, it is useful to consider a certain semi-phenomenological description of these new phases. In our previous paper [9], we proposed a thermodynamical approach for the description of antiferro- and ferri-electric chiral smectics with inclined molecules. This approach was related to the structures assumed for such smectics possessing complicated spatial director distributions $\Xi(z)$ along the crystalline z -axis. Function $\Xi(z)$ is, in fact, the sum of terms from so-called short pitch modes [10] (SPM with amplitudes θ_n and large wave numbers q_n) and the long pitch mode (LPM with amplitude θ_L and small wave number q_L). The n -SPM, in the absence of any incommensurability, describe pure antiferroelectric structures with unit cells along the z -axis, in which the projections of the two dimensional vector $\Xi(z)$ on the xy -plane have azimuthal distributions (stars) $\Xi(z_s)$ at points z_s corresponding to the coordinates of the smectic layers in the unit cell. In such a case, $q_n = k_n = m/nl$, where $m = 1, 2, \dots, n = \pm m, \pm(m+1), \dots, l$ is the thickness of a monomolecular layer, and the polarization vectors form closed manifold geometries

in the smectic planes, which correspond to various stars in n layers-unit cells. In the presence of a small incommensurability $\delta q_n = q_n - k_n$, the n -SPM describe weak ferrielectric states. In the case when SPM and LPM coexist, the ferrielectric properties must be very pronounced.

In the present paper, we shall describe various phase transitions and phase diagrams which are possible in the framework of the proposed model. It will be shown that, in fact, the families of phases are mainly managed by a few parameters. The nature of the so-called SmC_α^* phase and the reasons for its existence in a very narrow temperature interval near the point of phase transition to the SmA phase are discussed. The sequences of ferrielectric and antiferroelectric states (including the so called SmC_A^* phase and some intermediate states) are explained to be dependent on the interactions between the SPM and LPM. The induction and suppression of the long pitch mode by strong short pitch modes are described.

2. The thermodynamic conditions for the origin of SPM

In the simple approximation of non-interacting SPM, the free energy density F consists of spatially homogeneous and spatially heterogeneous parts. In this approximation, when only the terms quadratic in θ_j are taken into

* Author for correspondence.

† Part I see ref. [9]

account, we have

$$F = F^* + F_q = \sum_j F_j = \sum_j A_j \Theta_j^2 = \sum_j \left[\frac{R}{T_A} (T - T_j) + r f_j \right] \Theta_j^2 \quad (1)$$

where the positive constants R and r have the dimensions of coefficients A_j (i.e. of energy density), functions $f_j = f_j(\tau)$ are given by equations (14) and (16) and the referred temperature τ is given by (11) from [9]. It should be remembered that equation (1) is written for non-interacting j -modes, and therefore the magnitudes Θ_j are the only tilt angles at all points z_s in the unit cell for each mode. When the interactions between different modes are taken into account, the tilt angles at different points z_s in the unit cell become different for a given n -mode.

As mentioned in [9], temperatures T_j may be different if q_j are not exactly equal to k_j ($j = n$ and $T_j = T_n$ for the n -SPM), $T_j = T_L$ being also different for the long pitch mode with $q_j = q_L$ ($k_L = 0$), $T_j = T^*$ for $q_n = k_n$. For simplicity, it was assumed that the phenomenological parameter τ is equal to zero at the temperature T_A , at which the first phase transition from the smectic A to a chiral smectic with inclined molecules occurs, and, besides, increasing positive values of τ correspond to a decrease of T below T_A . In general, $T_n \neq T_A \neq T_L$, but the difference between these temperatures is much less than their values, i.e.

$$\tau \propto \frac{T_A - T}{T_A}. \quad (2)$$

Here, we shall continue to consider the case from [9] when the point $\tau(T_A) = 0$ may be slightly below point $\tau(T_{AC})$, i.e. temperature T_A is slightly higher than temperature of the phase transition to the chiral smectic C phase T_{AC} .

The appearance of the j -waves is determined by the coefficients A_j vanishing in the F_j terms at some points $T_{c,j}$. The magnitudes A_j are written as small positive values of τ in the form

$$A_n(\tau) = R \left[\frac{T_A - T_n}{T_A} - \left(1 + \frac{\pi |n|^3 \tilde{\beta} \alpha}{m^2} \right) \tau + \frac{\tilde{\beta}}{2} (n^3 \pi \tau)^2 \right] \quad (3)$$

$$A_L(\tau) \cong R \left[\frac{T_A - T_L}{T_A} - \frac{1}{2} \tilde{\beta} \alpha^2 + (\tilde{\beta} \alpha^2 v^{-1} \lambda^2 - 1) \tau \right] \quad (4)$$

where $\tilde{\beta} = 2r/R$. Because of the weakness of the incommensurability effects, it is reasonable to assume that all the magnitudes $(T_A - T_j)$ are small. The incommensurability effects, accordingly to equation (6) from [9], can effectively shift the transition temperatures similarly to the increase

in the temperature T_{CA} due to the existence of the conventional helix [11]. Figures 1–5 schematically show the temperature change of the parameters $A_j(\tau)$ below the temperature T_A for different arrangements of the $A_n(0)$ and $A_L(0)$ points.

It should be noted that the magnitudes $T_n(\delta q_n)$, according to equations (6) and (10) from [9], either increase with increasing number n when $n^3 \pi \gg m^2 \alpha v^{-1} \xi^2$ or decrease with increasing number n when $n^3 \pi \ll m^2 \alpha v^{-1} \xi^2$:

$$\delta T_n \equiv [T_n(\delta q_n) - T^*] \propto (\delta q_n)^2 \propto \left[\frac{|n|v}{m \xi^2} - \frac{m \alpha}{n^2 \pi} \right]. \quad (5)$$

In the example considered with $n \leq n_{\max} = 3$ at $m = 1$ (see figure 3 from [9]), for the 1 ($n = 1$)-, 2 ($n = -2$)- and 3 ($n = 3$)-SPM, we see from equation (5) that

$$T_1(\delta q_1) < T_2(\delta q_2) < T_3(\delta q_3) \quad \text{if} \quad \pi \gg \alpha v^{-1} \xi^2 \quad (6a)$$

$$T_3(\delta q_3) < T_2(\delta q_2) < T_1(\delta q_1) \quad \text{if} \quad 27\pi \ll \alpha v^{-1} \xi^2 \quad (6b)$$

the temperature inequalities being changed for different intervals of the $\alpha v^{-1} \xi^2$ values.

Temperature T_L , which formally corresponds to large values of $n \gg n_{\max}$, may be larger than all the temperatures $T_n(\delta q_n)$, i.e. $T_A < T_L$, $(T_A - T_L)$ is of the order of $(-\tilde{\beta} \alpha^2 T_A)$. For the conditions (6a), T_A is close to T_3 , $(T_A - T_3)$ is of the order $(T_A v^2 / \xi^4)$; $(T_A - T_2) \cong 6 T_A v^2 \xi^{-4}$; $(T_A - T_1) \cong 9 T_A v^2 \xi^{-4}$. These assumptions (as a model) correspond to the observed increase in the phase transition temperatures when the period of the structures increases and they are useful for further estimations. For other conditions, for instance (6b), the considerations are quite similar.

Equation (4) shows that the line $A_L(\tau)$ has a positive slope under the condition

$$(\tilde{\beta} \alpha^2 v^{-1} \lambda^2 - 1) \geq 0 \quad (7)$$

but this slope is negative for the inverse inequality. The first case is probable for sufficiently large values of the correlation length λ , because of the small values of the parameter $\alpha \beta$. For simplicity, we shall assume that $\tilde{\beta} \alpha^2 \lambda^2 \geq v$, i.e. the line $A_L(\tau)$ has a weak positive slope. Function $A_L(\tau)$ has a zero value at $\tau = \tau_L^0$,

$$\tau_L^0 = \frac{\tilde{\beta} \alpha^2}{2(\tilde{\beta} \alpha^2 v^{-1} \lambda^2 - 1)} \quad (8)$$

which can be relatively large.

Now, by equation (2), we can describe the changes of functions $A_j(\tau)$ dependent on the material parameters $\tilde{\beta}$, α and ξ . Near the T_A point, the $A_3(\tau)$ line has a narrow local minimum. $A_3(\tau)$ is equal to zero at the points

$$\tau_3^{\theta 1} \cong \frac{v^2 \xi^{-4}}{1 + \tilde{\beta}(27\pi \alpha)} \quad \text{and} \quad \tau_3^{\theta 2} \cong \frac{2\alpha}{27\pi} + \frac{2}{\tilde{\beta}(27\pi)}. \quad (9)$$

In such a case, function $A_3(\tau)$ has a negative value at the minimum

$$A_{3\min}/R \cong v^2 \xi^{-4} - \frac{(1 + \tilde{\beta} 27\pi\alpha)^2}{2\tilde{\beta}(27\pi)^2} \quad (10)$$

at the point

$$\tau_{3\min} \cong \frac{1 + \tilde{\beta} 27\pi\alpha}{\tilde{\beta}(27\pi)^2}. \quad (11)$$

The τ_3^{01} and τ_3^{02} values may be of the same order of value at sufficiently small ξ , and, in such a case, the negative value at the minimum disappears.

The corresponding values for function $A_1(\tau)$ and $A_2(\tau)$ are

$$\tau_1^{01} \cong \frac{9v^2 \xi^{-4}}{1 + \tilde{\beta} \pi\alpha}, \quad \tau_1^{02} \cong \frac{2\alpha}{\pi} + \frac{2}{\tilde{\beta}\pi^2}, \quad \tau_{1\min} \cong \frac{1 + \tilde{\beta} \pi\alpha}{\tilde{\beta}\pi^2},$$

$$A_{1\min}/R \cong 9v^2 \xi^{-4} - \frac{(1 + \tilde{\beta} \pi\alpha)^2}{2\tilde{\beta}\pi^2}; \quad (12)$$

$$\tau_2^{01} \cong \frac{6v^2 \xi^{-4}}{1 + 8\tilde{\beta}\pi\alpha}, \quad \tau_2^{02} \cong \frac{\alpha}{4\pi} + \frac{1}{32\tilde{\beta}\pi^2}, \quad \tau_{2\min} \cong \frac{1 + 8\tilde{\beta}\pi\alpha}{8\tilde{\beta}\pi^2},$$

$$A_{2\min}/R \cong 6v^2 \xi^{-4} - \frac{(1 + 8\tilde{\beta}\pi\alpha)^2}{16\tilde{\beta}\pi^2}. \quad (13)$$

The value $A_{1\min}$ is negative at larger values of the correlation length (with respect to the cases of $A_{2\min}$ and $A_{3\min}$), and besides, $|A_{1\min}|$ is smaller than these at the same ξ value. In the presence of both negative minima values, for relatively large ξ , the lines $A_1(\tau)$ and $A_3(\tau)$ intersect at $\tau = \tau_{31}$,

$$\tau_{31} \approx \frac{2\alpha}{27\pi} \quad (14)$$

$$A_1(\tau_{31})/R = A_3(\tau_{31})/R \cong \frac{9v^2}{\xi^4} - \frac{2\tilde{\beta}\alpha}{27} \quad (15)$$

and the latter value is negative for the condition $\tau_3^{02} \geq \tau_1^{01}$. For sufficiently large ξ , we have the inequalities

$$|A_1(\tau_{31})| = |A_3(\tau_{31})| \approx \frac{2\tilde{\beta}\alpha}{27} R. \quad (16)$$

The value $A_L(\tau_{31})$, according to equation (3), is close to the $A_L(0)$ value. The $A_L(\tau_{31})$ and $A_1(\tau_{31}) = A_3(\tau_{31})$ values have the same order of value at $\alpha \sim 1/10$. Since the negative $A_{1\min}$ value appears for the condition

$$\frac{\alpha}{2\pi} + \frac{1}{2\tilde{\beta}\pi^2} \geq \frac{9v^2 \xi^{-4}}{1 + \tilde{\beta}\pi\alpha} \quad (17)$$

we see from the inequalities $\tau_3^{02} \geq \tau_1^{01}$ and (17) that, for decreasing correlation length ξ , the intersection of lines $A_1(\tau)$ and $A_3(\tau)$ first disappears and then, for smaller values of ξ the negative $A_{1\min}$ value vanishes.

Similar calculations show that the intersections of lines $A_1(\tau)$ and $A_2(\tau)$ and of lines $A_2(\tau)$ and $A_3(\tau)$ occur, respectively, at $\tau = \tau_{21}$ and $\tau = \tau_{23}$, where

$$\tau_{21} \leq \cong \frac{\alpha}{4\pi}, \quad A_1(\tau_{21}) = A_2(\tau_{21}) \approx \frac{9v^2}{\xi^4} - \frac{\alpha}{4\pi} \quad (18)$$

$$\tau_{23} \approx \frac{2\alpha}{35\pi}, \quad A_3(\tau_{23}) = A_2(\tau_{23}) \approx \frac{v^2}{\xi^4} - \frac{2\alpha}{35\pi}. \quad (19)$$

For relatively small α , we obtain

$$\tau_{31} \approx \frac{4v}{27\pi\sqrt{\tilde{\beta}\xi^2}}, \quad \tau_{21} \approx \frac{\sqrt{6}v}{8\pi\sqrt{\tilde{\beta}\xi^2}}, \quad \tau_{23} \approx \frac{\sqrt{2}v}{\pi\sqrt{133\tilde{\beta}\xi^2}}. \quad (20)$$

In general, the intersections 31, 21 and 23 occur at negative values of the amplitudes $A_j(\tau_{ij})$ if the following conditions are fulfilled:

intersection 31 occurs at $\tau_3^{02} \geq \tau_1^{01}$,

intersection 21 occurs at $\tau_2^{02} \geq \tau_1^{01}$,

intersection 23 occurs at $\tau_3^{02} \geq \tau_2^{01}$.

Thus, at sufficiently small α and at not very large ξ , the latter inequalities may be broken and such intersections become impossible. These examples, (8)–(20), show that the chirality parameter and correlation length control and mutual arrangement of SPM and LPM branches which can differ from the simple picture shown in figure 3 from [9].

3. The effects of intermode interactions on phase diagrams

To study the characters, sequence and temperatures of the phase transitions under consideration, we should take into account the more complicated expression for F :

$$F = \sum_j F_j = \sum_j A_j \Theta_j^3 + \frac{1}{2} \sum_j B_j \Theta_j^4 - \frac{1}{2} \sum_{h \neq j_2} v_{1j_2} \Theta_{j_1}^2 \Theta_{j_2}^2 \quad (21)$$

where positive B_j are assumed to be of the same order of value ($B_j \approx B$), and v_{1j_2} are the constants of the intermode interactions. The interaction terms may be negative (the v_{1j_2} coefficients may be positive), and this means that such interactions induce the appearance of both the modes. To see the effects of these interactions in detail, we should consider various possible sets of lines $A_j(\tau)$, the zero points, intersection points and the points of minima of such functions and their dependence on the basic parameters α and ξ .

According to the results obtained above, we can present now, in the framework of the model, the general picture of the phase transitions in chiral liquid crystalline

materials with various values of correlation length. First of all, in materials which do not have large ξ values, function $A_L(\tau)$ has definitely a negative slope, and all the functions $A_n(\tau)$ (in fact, $n = 1$) have positive minima values. This means that, in such materials we can only observe the phase transition SmA–SmC*, see figure 1(a). In fact, the smectic phase with inclined molecules cannot exist at very low temperatures (at large values of τ), i.e. there is a phase transition either into a crystalline phase or into a low symmetry smectic phase at a certain value $\tau = \tau_{lim}$. In the problem under consideration, we have the limit value of the order of $\tau_{lim} \propto \alpha/\pi$ above which the energies of all the n -SPM become large, and the existence of the long pitch mode might also be unfavourable above $\tau = \tau_{lim}$.

At a larger value of ξ , the slope of the line $A_L(\tau)$ becomes positive, but, if the lines $A_n(\tau)$ lie above the τ axis, we can only observe again the SmC* phase, see figure 1(b). In figures 2 and 3, the $A_n(\tau)$ lines shown have, in fact, no physical sense if $\xi \cong 1$. With increasing ξ , the first line $A_1(\tau)$, describing the physically existing 1-SPM ($n_{max} = 1$), appears, the first negative minimum value A_{1min} also appears, and the line $A_L(\tau)$ intersect the τ axis at values $\tau \gg \tau_{lim}$, see figure 2(a).

If the L- and 1-SPM waves should not interact between themselves, figure 2(a) could describe the second order phase transitions SmA–SmC* at the point $\tau(T_{AC})$ and also the transition SmC* to a ferroelectric phase (FI state as a coexistence of the long pitch mode and 1-SPM) at the point $\tau(T_{C^*/FI}) = \tau_1^1 \leq \tau_{lim} \cong \alpha/\pi$. If the above mentioned value $\tau = \tau_{lim}$ is of the order of α/π , we can observe the phase transition FI to a crystalline state

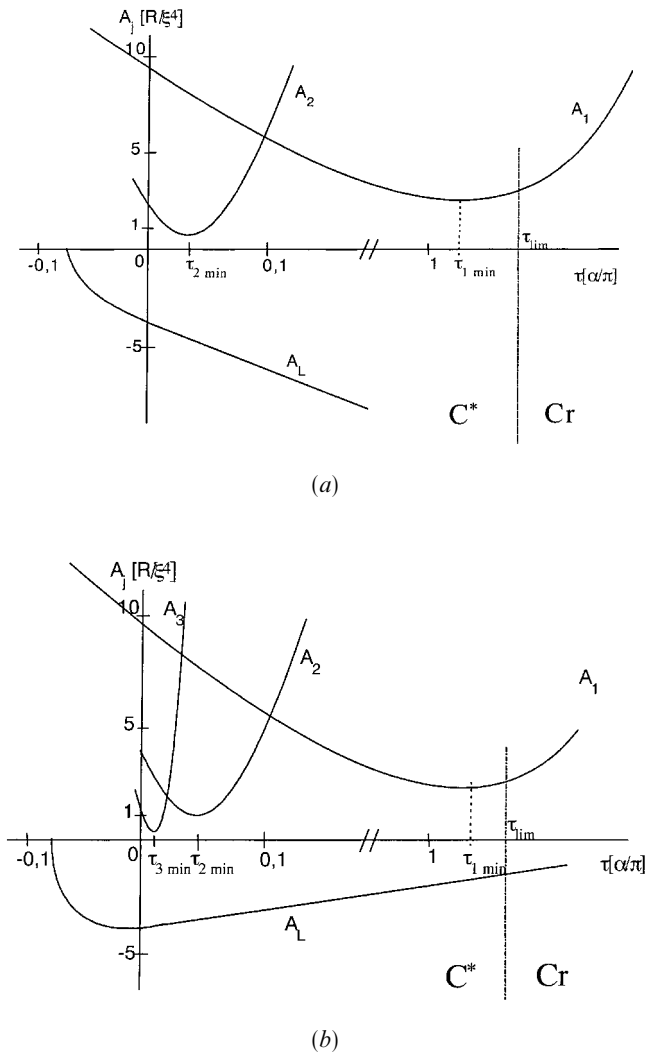


Figure 1. The SPM and LPM branches of energy as functions of reduced temperature for smectics with a small correlation length ξ . Only the SmA–SmC* phase transition occurs, and sets (a) and (b) show the change of slope of function $A_L(\tau)$ at increasing ξ .

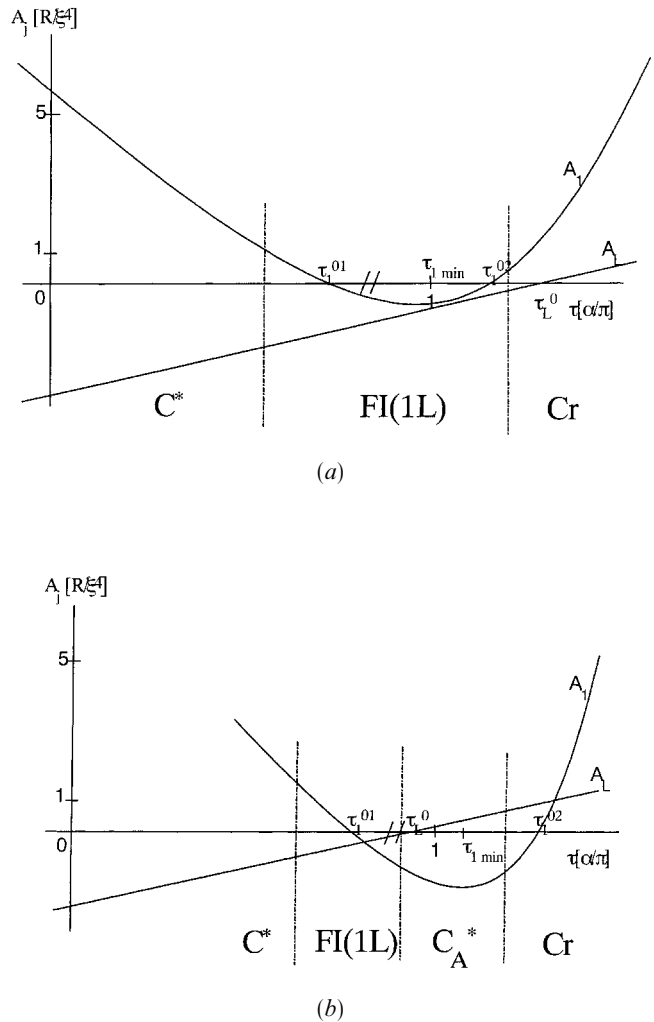


Figure 2. The $A_L(\tau)$ and $A_1(\tau)$ branches for smectics with a larger ξ , when the first negative minimum A_{1min} appears: (a) the SmC* and ferroelectric phases occur, (b) the antiferroelectric phase arises at increasing $A_3(\tau)$.

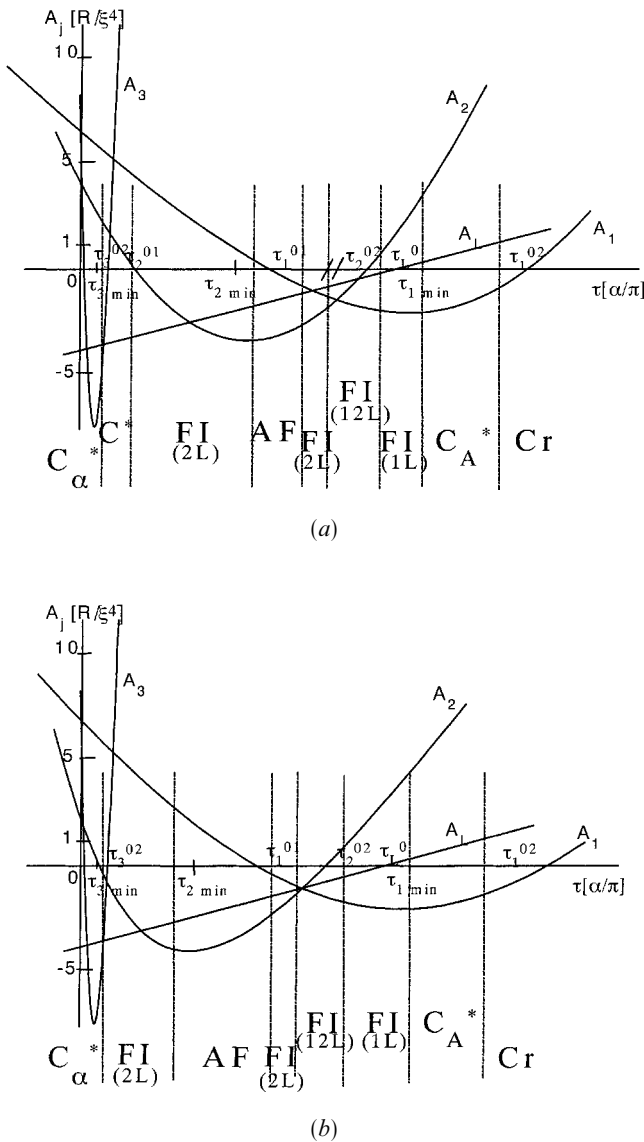


Figure 3. Three SPM [branches $A_1(\tau)$, $A_2(\tau)$, and $A_3(\tau)$] provide the appearance of several ferri- and antiferroelectric phases in smectics with large ξ . A strong mixing of LPM and 3-SPM in a narrow temperature interval near the $\tau = 0$ point results in the appearance of a specific ferrielectric phase. In an intermediate τ interval, where the weight of LPM is small with respect to the weight of 2-SPM, a new almost antiferroelectric phase arises. Sets (a) and (b) show the disappearance of the SmC^* phase at increasing ξ .

at such a temperature (at the point $\tau(T_{F1/Cr})$). The interaction ($-\nu$) between the L- and 1-SPM waves shifts the real phase transition points. For instance, at small values of ν , the point $\tau(T_{C^*/FI})$ is determined by the equation

$$BA_1(\tau) = -\nu A_L(\tau) \quad (22)$$

and shifts to larger temperatures with increasing ν . At $\nu > B$, the $\text{C}^*\text{-FI}$ phase transition becomes first order and,

at ν close to B , the shift of $\tau(T_{C^*/FI})$ becomes essential since $A_1(\tau) \cong -A_L(\tau)$ in such a case. The same conclusion can be reached for the point $\tau(T_{FI/Cr}) = \tau_1^{02} \geq \tau_{1\min} \cong \alpha/\pi$ which shifts to lower temperatures with increasing ν , see figure 2(a).

If parameter ξ is slightly larger than in the previous case (in the presence of only 1-SPM) when, at $\tilde{\beta}\alpha^2\xi^2 > 1$, magnitudes $A_L(0)/R \cong -\tilde{\beta}\alpha^2/2$ and $A_{1\min}$ are comparable in their values and line $A_L(\tau)$ has a larger slope, we obtain the situation shown in figure 2(b): line $A_L(\tau)$ intersects the τ -axis at the point τ_L^0 which is in between points τ_1^{01} and τ_1^{02} . In such a case, we can observe the phase transitions $\text{SmC}^*\text{-FI}$ at the point $\tau(T_{C^*/FI}) \cong \tau_1^{01}$, FI to an antiferroelectric phase (denoted SmC_A^* for the 1-SPM) at the point $\tau(T_{FI/C_A^*}) \cong \tau_L^0$, and $\text{SmC}_A^*\text{-Cr}$ at a lower temperature if the interaction constant ν is small.

At $\nu > B$, the corresponding points for the first order phase transitions shift similarly to those of the previous case: $\tau(T_{C^*/FI})$ shifts to higher temperatures in accordance with equation (22) and $\tau(T_{FI/C_A^*})$ shifts to lower temperatures accordingly to the equation $BA_L(\tau) = -\nu A_1(\tau)$. It should be noted that the equation $A_1(\tau) \cong -A_L(\tau)$ may induce relatively large shifts of the transitions points since the values $A_L(0)$ and $A_{1\min}$ are comparable, i.e. the slopes of lines $A_1(\tau)$ and $A_L(\tau)$ are small. In the FI phase, where the LPM coexists with the 1-SPM, the weight, i.e. the amplitude, of LPM continuously decreases with decreasing temperature. Due to hysteresis phenomena, there are temperature ranges of coexistence of different modes in the vicinities of the first order phase transition points.

At a larger value of ξ , several SPM could appear, and the observable SPM is only one of them, for example the 2-SPM, if other parameters ($\tilde{\beta}$ and α) are not appropriate for the existence of negative values of magnitude $A_1(\tau)$. Now, the situation shown in the figures 2 is repeated for the 2-SPM with the same sequence of phase transitions, but over a more narrow temperature interval.

In materials with larger values of ξ , i.e. with a larger number $n_{\max} \sim \xi/2$, the 2-SPM, 3-SPM, etc. modes appear. Let us imagine that the number of SPM is equal to 3. In accordance with results shown above, the $A_j(\tau)$ branches for all the modes are presented by the figures 3 as functions of increasing values of ξ . The larger ξ , the deeper are the minima of the SPM, the intersections of which begin to take place at negative values of $A_j(\tau)$, the minima of SPM with larger numbers being deeper. The slope of line $A_L(\tau)$ becomes larger at the same time. It is seen that $\tau_{3\min}$ is very close to the point $\tau(T_A) = 0$ and thus to the point $\tau(T_{AC})$. The relatively strong interaction between the LPM and 3-SPM may strongly shift the first temperature towards the latter one, especially at the first order transition. Thus, for materials with sufficiently large correlation lengths, there is an obvious

mixing (coexistence) of the two modes in close proximity to the $\tau(T_A)$ point. Therefore, the existence of a specific ferrielectric phase in the vicinity of the $T_A \cong T_{AC}$ temperature is very probable in such a case. We can consider this FI state as the so called SmC_α^* phase. It should be noted that, for the condition $\xi^2 \gg 1$, the first zero point τ_2^{01} of function $A_2(\tau)$ can also be close to the $\tau(T_A)$ point [see equation (13)], i.e. in general several modes can coexist in the narrow temperature interval ascribed to the SmC_α^* temperature range.

Since lines $A_2(\tau)$ and $A_L(\tau)$ intersect at negative values of these functions before (with ξ increasing) the intersection of lines $A_2(\tau)$ and $A_3(\tau)$ at negative values of the latter functions, we obtain the situation shown in figure 3(a) when line $A_L(\tau)$ intersects all the SPM lines $A_1(\tau)$, $A_2(\tau)$ and $A_3(\tau)$. In this case, we see that the existence of the SmC_α^* , SmC^* , several FI and the SmC_α^* phases is very probable in the respective temperature intervals. Strictly speaking, there is only one antiferroelectric phase (SmC_α^*) in such a model because the other states include LPM, but LPM has different weights (amplitudes) in each of these states. For instance, in the SmC_α^* phase the weights of different modes are comparable; but in the FI phases, the weights of LPM and various SPM essentially differ for different temperature intervals (see figures 3).

It is seen in figures 3 that in the vicinity of the $\tau_{3\min}$ point, dependent on the values of the material parameters, the magnitude $|A_L(\tau_{2\min})|$ may be rather smaller than the magnitudes $|A_2(\tau_{2\min})| = |A_{2\min}|$, whereas in the vicinity of the τ_{21} point, the amplitudes $|A_L(\tau_{21})|$ and $|A_2(\tau_{21})| = |A_1(\tau_{21})|$ may be comparable at sufficiently large values of ξ and for a strong chirality α , see equations (3) and (18). In such a situation, in a temperature interval near the $\tau_{2\min}$ point, the weight of LPM is rather smaller than the weight of 2-SPM, and this state may be experimentally classified as an antiferroelectric state (the AF phase). In another temperature interval, near the τ_{21} point, the weights of LPM, 1-SPM and 2-SPM are comparable—we denote this state as the FI(12L) state. Similarly, near the τ_2^{02} point, LPM and 1-SPM have larger weights—the FI(1L) state; but, near the τ_1^{01} point, LPM and 2-SPM have larger weights—the FI(2L) state. Thus, in between the so called AF and SmC_α^* states, three FI states can exist. It should be noted that near the intersection point of the $A_L(\tau)$ and $A_2(\tau)$ lines τ_{2L} , if it is sufficiently far from the $\tau = 0$ point, the existence of the FI(2L) state (but only one FI state) is probable.

It is useful to discuss the role of intermode interactions for such complicated phase diagrams. Let us consider, for example, the interaction of LPM and n -SPM, taking into account not only the weak negative third term in equation (21) but also positive terms of a higher order,

for instance in the form

$$-\frac{1}{2}v\vartheta_L^2\vartheta_n^2 + w\vartheta_L^2\vartheta_n^4 \quad (23)$$

where positive constant v is much less than positive constant w . Thus, if LPM (as a secondary mode) is induced by the n -SPM mode, the effective interaction for such an induction is $(-\sqrt{2}) + w\vartheta_n^2$. The latter term is negative if the leading ϑ_n amplitude is small, but the effective interaction is positive if the ϑ_n amplitude is larger than $(\sqrt{2}w)^{1/2}$. This means that if, at the point of intersection of the $A_L(\tau)$ and $A_n(\tau)$ lines, the ϑ_n amplitude is sufficiently larger, then in fact the induction of LPM is impossible and, therefore, this mode is suppressed. In the latter case, a real antiferroelectric state (as the n -SPM) could arise.

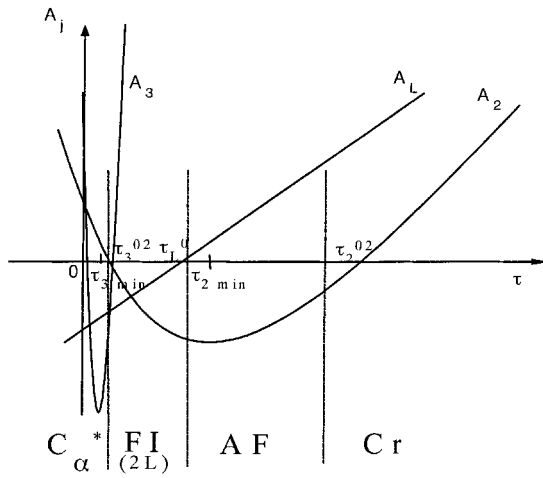
The values $A_L(0)$ and $A_n(0)$ are of great importance for the existence of the ‘families’ of phase transitions. If the shifts δT_i are very small at large values of ξ we can expect the situation shown in the figures 4, where the τ_2^{01} value is very close to zero and the slope of line $A_L(\tau)$ is relatively large. Dependent on these characteristics, we obtain the following cases of sequences of phase transitions: (a) $\text{SmA}-\text{SmC}_\alpha^*-\text{FI}-\text{AF}$, (b) $\text{SmA}-\text{SmC}_\alpha^*-\text{AF}$, (c) $\text{SmA}-\text{AF}$.

The values $A_n(0)$ may change the sequence $A_3(0) < A_2(0) < A_1(0)$ if the inequality $n^3\pi \leq \alpha\xi^2$ takes place, since the sequence of the temperatures $T_n(\delta q_n)$ changes in such a case. For instance, for sufficiently large chirality and correlation length, the inequalities $A_3(0) < A_1(0) < A_2(0)$ occur, and, correspondingly the inequalities $A_{3\min} < A_{1\min} < A_{2\min}$ may take place. In this case, the sequence of intersections of lines $A_j(\tau)$ also changes (see figure 5), and we should expect a change of phase diagram.

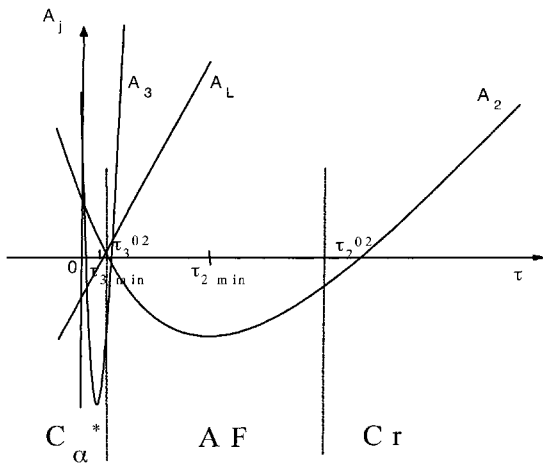
If magnitude ξ is sufficiently large, the $A_2(\tau)$ and $A_3(\tau)$ curves also intersect at negative values of these functions [see figure 3(b)], the moduli of these values being much less than magnitude $|A_L(\tau_{32})|$ in the vicinity of the τ_{32} point. Thus, in such a case the SmC^* phase disappears, but appearance of the ferrielectric phase FI(23L) occurs which has small weights of short pitch modes. We can write the relaxations between corresponding amplitudes ϑ_L , ϑ_2 and ϑ_3 in the form

$$\vartheta_L \cong \left[\frac{|A_L(\tau_{32})|}{B} \right]^{1/2} \gg \vartheta_2 \cong \vartheta_3 \cong \left[\frac{|A_2(\tau_{32})|}{B} \right]^{1/2}. \quad (24)$$

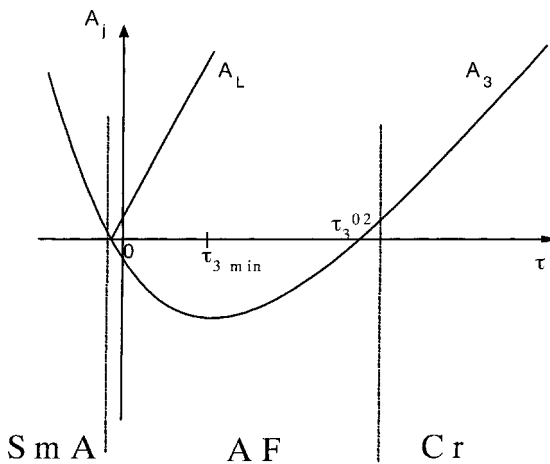
To observe the SmC^* phase, the weak SPM should be eliminated by the external electric field E which eliminates the short pitch wave above a certain threshold



(a)



(b)



(c)

Figure 4. The sets (a), (b) and (c) of SPM and LPM at large ξ and small shifts δT_j provide the change in the phase diagrams.

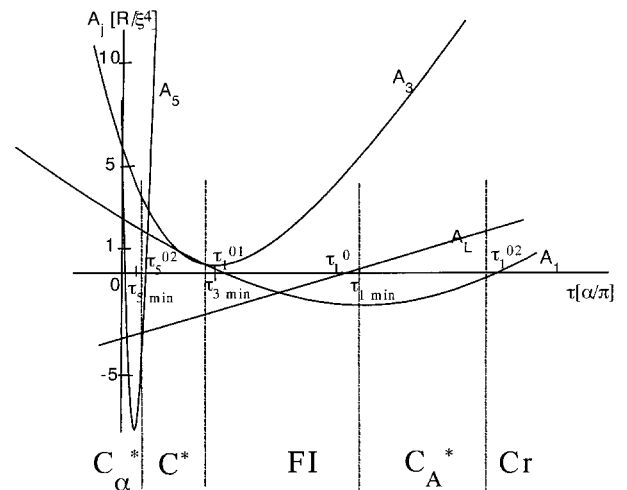


Figure 5. The phase diagram for a different set of shifts δT_j .

$E_{th,n}$, for example,

$$E_{th,3} \propto \frac{r\beta\alpha^2 \Theta_3}{\mu}, \quad E_{th,2} \propto \frac{r\beta\alpha^2 \Theta_2}{\mu}, \quad (25)$$

where μ is the piezoelectric constant. These relations remind one of conventional relations in which the magnitude of the order of Kq^2 is instead that of $r\beta\alpha^2$, where K is the elastic constant. In the case under consideration, we obtain estimates (25) from the condition which corresponds to the equality (in the order of values) $A_{jmin} \Theta_j^2 \propto -\mu \Theta_j E$, where $|A_{jmin}| \propto r\beta\alpha^2$, $\mu \Theta_j \propto P_j$ is the polarization of the j -mode, and $r\beta\alpha^2 \gg Rn^2 v^2 \xi^{-4}$. If $|A_{jmin}| \propto Rv^2 \xi^{-4}$ for some materials, then $E_{th,j} \propto R\mu^{-1} v^2 \xi^{-4} \Theta_j$. Thus, small amplitudes of SPM allow elimination of such weak short pitch waves and restoration of the SmC* phase or a certain FI state and simultaneously the elimination of other FI and AF states. It is also possible to amplify a weak LPM by an electric field (to increase the Θ_L amplitude) and thus to induce a hidden FI state.

4. Conclusions

It is shown that the families of phases are mainly controlled by three parameters: correlation length ξ , chirality α and a heterogeneous term to homogeneous term ratio in free energy r/R . These parameters effectively change the positions of SPM and LPM branches at the phase plane energy/temperature, and thus they determine the appearance of various phase sequences. The larger these parameters are, the more favourable is the appearance of antiferro- and ferri-electric phases related to SPM and the less favourable is the existence of the SmC* phase at lower temperatures. The number of SPM increases with increasing ξ . The real maximum number

of various ferroelectric and antiferroelectric states is close to 10. The so called SmC_o^* phase is a mixture of several short pitch waves with the largest pitches, and it occurs, in general, in a very narrow temperature interval near the point of phase transition to the SmA phase. In the temperature scale, there are up to three ferroelectric phases between two possible antiferroelectric phases, the ferroelectric states being described as the obvious coexistence of long pitch and several short pitch modes. The so called SmC_A^* phase, existing at the lowest temperatures, is the short pitch mode with the shortest pitch. But antiferroelectric states as short pitch modes with a larger pitch also occur.

In general, ferroelectric phases may exist not only in the presence of LPM, but also due to the inherent incommensurability of SPM. In such a sense, the pure antiferroelectric states are not numerous, and it is better to talk about weak ferroelectric states. The latter also occur when the LPM present has a small amplitude. The existence of either of the two possibilities for the long pitch mode, its induction by an electric field and its suppression by strong short pitch modes, is demonstrated.

Financial support from the Deutsche Forschungsgemeinschaft is gratefully acknowledged; S. P. and M. G.

are grateful to the Russian Foundation of Fundamental Research (grant 98-02-16802). We also thank J. K. Vij for fruitful discussions of the experimental results and theoretical aspects.

References

- [1] FUKUDA, A., TAKANISHI, Y., ISOZAKI, T., ISHIKAWA, K., and TAKEZOE, H., 1994, *J. mater. Chem.*, **4**, 997.
- [2] TAKANISHI, Y., HIRAOKA, K., AGRAWAL, V., TAKEZOE, H., FUKUDA, A., and MATSUSHITA, M., 1991, *Jpn. J. appl. Phys.*, **30**, 2023.
- [3] ISOZAKI, T., FUJIKAWA, T., TAKEZOE, H., FUKUDA, A., HAGIWARA, T., SUZUKI, Y., and KAWAMURA, I., 1992, *Jpn. J. appl. Phys.*, **31**, 1435.
- [4] HIRAOKA, K., TAKANISHI, Y., SHARP, K., TAKEZOE, H., and FUKUDA, A., 1991, *Jpn. J. appl. Phys.*, **30**, L1819.
- [5] ORIHARI, H., and ISHIBASHI, Y., 1990, *Jpn. J. appl. Phys.*, **29**, L115.
- [6] ZEKS, B., and CEPIC, M., 1993, *Liq. Cryst.*, **14**, 445.
- [7] LORMAN, V. L., BULBITCH, A. A., and TOLEDANO, P., 1994, *Phys. Rev. E*, **49**, 1367.
- [8] CEPIC, M., and ZEKS, B., 1995, *Mol. Cryst. liq. Cryst.*, **263**, 61.
- [9] PIKIN, S. A., GORKUNOV, M. V., KILIAN, D., and HAASE, W., 1991, *Liq. Cryst.*, **26**, 1107.
- [10] PIKIN, S. A., HILLER, S., and HAASE, W., 1995, *Mol. Cryst. liq. Cryst.*, **262**, 425.
- [11] PIKIN, S. A., 1991, *Structural Transformations in Liquid Crystals* (New York: Gordon & Breach Science Publishers).